Robot Dynamic Model Identification Through Excitation Trajectories Minimizing the Correlation Influence among Essential Parameters

Enrico Villagrossi[1,2], Giovanni Legnani[2], Nicola Pedrocchi[1], Federico Vicentini[1], Lorenzo Molinari Tosatti[1], Fabio Abbà[3] and Aldo Bottero[3]

[1] *Institute of Industrial Technologies and Automation, National Research Council, via Bassini 15, 20133 Milan, Italy*

[2] *University of Brescia, Dep. of Mechanical and Industrial Engineering, via Branze 39, 25123 Brescia, Italy*

[3] *COMAU Robotics, via Rivalta 30, Grugliasco (TO), Italy*

Keywords: Industrial Robot Dynamics Identification, Optimal Excitation Trajectories, Dynamics Decoupling.

Abstract: Robot dynamics is commonly modeled as a linear function of the robot kinematic state from a set of dynamic parameters into motor torques. Base parameters (*i.e.* the set of theoretically demonstrated linearly-independent parameters) can be reduced to a subset of "essential" parameters by eliminating those that are negligible with respect to their contribution in motor torques. However, generic trajectories, if not properly defined, couple the contribution of such essential parameters into the motor torques, actually reducing the estimation accuracy of the dynamics parameters. The work presented here introduces an index for evaluating correlation influence among essential parameters along an executed trajectory. Such index is then exploited for an optimal search of excitatory patterns consistent with the kinematical coupling constraints. The method is experimentally compared with the results achievable by one of the most popular IRs dynamic calibration method.

1 INTRODUCTION

Model-based strategies have been introduced in industrial robots (IRs) control since three decades. Nonetheless, in spite of the vast literature, methods for the identification of the dynamic parameters still remain a matter of substantial investigation.

In fact, an *a priori* knowledge of the robot dynamic parameters is often unavailable (*e.g.* CAD data obtained from the design data of manipulators) and weight tolerances of robot links are remarkable due to the inaccuracy of the casting process (*e.g.* around 5-10%, mean value provided by different IR manufacturer). Additionally, the real friction model identification is an experimental procedure *per se*, with parameters varying along production batches and time.

In pioneering works (Atkeson et al., 1986; Gautier and Khalil, 1988), the analysis of energy models led to the identification of a *base* sub-set of parameters (BP) that are observable through the measure of motor torques and positions. However, (Pham, 1991) experimentally demonstrated that only a smaller subset of *essentials* parameters (EP) are really significant, *i.e.* their contribution is not influenced by the precision and the noise of measuring systems. The set of EP is valid over and can be numerically computed in the entire workspace (Antonelli et al., 1999).

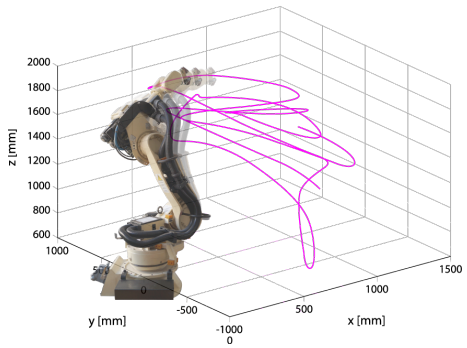

Figure 1: Identification Trajectories.

Different identification procedures for EP have been proposed in literature (Wu et al., 2010). In general, the common purpose is to identify the set of dynamic parameters that minimizes torque prediction errors (see Section 2 for analytical details). The identification requires an "optimal" trajectory able to excite to the best of some metrics the torque produced by the parameters to be identified (Swevers et al., 1997; Indri et al., 2002; Park, 2006), see Figure 1. The definition of "most exciting" trajectory is not unique, and three main issues have to be faced: (i) the identifica-

Villagrossi E., Legnani G., Pedrocchi N., Vicentini F., Molinari Tosatti L., Abbà F. and Bottero A..
Robot Dynamic Model Identification Through Excitation Trajectories Minimizing the Correlation Influence among Essential Parameters.
DOI: 10.5220/0005060704750482
In *Proceedings of the 11th International Conference on Informatics in Control, Automation and Robotics* (ICINCO-2014), pages 475-482
ISBN: 978-989-758-040-6

tion of metrics for evaluating the excitation capability; (ii) the consistent comparison of trajectories with different time-spans; (iii) the selection of the class of trajectory to be used for robot dynamic excitation.

About the metrics, two indexes (and their combinations) are mainly used for quantifying the excitatory power (Presse and Gautier, 1993; Pukelsheim, 2006; Wu et al., 2010): the determinant of the dynamic regressor (*i.e.* estimation with minimal uncertainty bounds); the conditioning number of the dynamic regressor (for minimizing the bias of estimates due to un-modeled dynamics errors). Such kind of metrics derive from standard mathematic techniques used in the analysis of observability of linear systems. However, these methodologies do not allow to overcome the limitations in observability of EP (Gautier and Venture, 2013). In fact, both metrics could be ideally reliable in case of constant uncorrelated excitation of parameters along the full trajectory, which is never the case: for a generic instant time of a generic trajectory the complete set of the EP should be not observable, and the coupling of the parameters should vary during the trajectory execution. The second key-aspect in trajectory selection, poorly investigated in literature, is that standard metrics (*e.g.* the determinant of the regressor) depend on the number of samples of the trajectory. A common solution consists in extracting an equal number of points from different trajectories. However, the coupling in robot dynamics does not maintain a constant rate, so differently down-sampled trajectories may fail in reproducing the coupling effects. The selection of trajectory classes has instead been deeply investigated in literature, because it is interpreted as the main tool for improving the estimation procedure. Many examples of trajectories have been considered for the proper excitation of the dynamics (*e.g.* 5^{th} order polynomials in (Caccavale and Chiacchio, 1994), splines in (Rackl et al., 2012), a combination of cosine and ramp in (Otani and Kakizaki, 1993), finite sums of harmonic sine and cosine in (Swevers et al., 1997), *etc.*). However, (Villagrossi et al., 2013) displays the limited extrapolation power of classes of excitatory trajectories and how the estimation of EP is affected by such classes: estimated parameters provide a high prediction power only over trajectories of the same family of those used during estimation.

The here presented identification method, attempts to overcome all the three issues reported in the standard methods. First, an index derived from the conditioning number index (Presse and Gautier, 1993) is introduced for the evaluation of the coupling effect in robot dynamics along a trajectory. Second, a scaling factor over the samples size is introduced for the determinant of the robot dynamics linearized regressors, in order to align for comparison different trajectories, preserving all the sampled dynamics. Last, the excitatory method is an extension of the approach in (Villagrossi et al., 2013) to the whole joint workspace. The method employs at identification time a template-class of trajectories applied in most manufacturing tasks, *i.e.* general trajectories described by a set of discrete poses to be interpolated by the built-in IR motion planner on the basis of global user-tunable parameters (fly-by accuracy, velocity profiles, *etc.*)[1].

Notation

$\mathbf{q} = \left[q^1, .., q^{dof}\right]^t$**:** Joint positions.

$\mathbf{q}_{t_k}, \dot{\mathbf{q}}_{t_k}, \ddot{\mathbf{q}}_{t_k}, \boldsymbol{\tau}_{t_k}$**:** Joint Positions Velocities, accelerations, torques at k-th sample time.

$\tilde{(\cdot)}, \hat{(\cdot)}, (\cdot)^*$**:** Measured, estimated value and optimum estimation respectively.

$(\cdot)^+$**:** is the Moore-Penrose Pseudo-inverse.

2 PROBLEM FORMALIZATION

The robot dynamics at time t_k is commonly reduced (Gautier and Khalil, 1988) to:

$$\boldsymbol{\tau}_{t_k} = \boldsymbol{\phi}\left(\ddot{\mathbf{q}}_{t_k}, \dot{\mathbf{q}}_{t_k}, \mathbf{q}_{t_k}\right)\boldsymbol{\pi}, \tag{1}$$

where $\boldsymbol{\pi}$ is the set EP and matrix function $\boldsymbol{\phi}$ is a generalized accelerations. $\boldsymbol{\pi}$ includes only combination of parameters that are experimentally observable along any excitatory trajectory that generates $\boldsymbol{\phi}$. The minimal size N_π of $\boldsymbol{\pi}$ depends on the robot kinematic topology (Presse and Gautier, 1993; Antonelli et al., 1999). In addition, other N_f coefficients of the friction model yield the compound parameters set $\boldsymbol{\pi}$. The selected friction model (Indri et al., 2002) provides the j-th joint friction torque function of three parameters, f_0^j, f_1^j, f_2^j as:

$$\tau_f^j = f_0^j \operatorname{sign}(\dot{q}^j) + f_1^j \dot{q}^j + f_2^j \operatorname{sign}(\dot{q}^j)\left(\dot{q}^j\right)^2.$$

For a trajectory of S-samples eq. (1) is expanded as:

$$\mathbf{T}_S \equiv \begin{bmatrix} \boldsymbol{\tau}_{t_1} \\ \vdots \\ \boldsymbol{\tau}_{t_S} \end{bmatrix} = \begin{bmatrix} \boldsymbol{\phi}\left(\ddot{\mathbf{q}}_{t_1}, \dot{\mathbf{q}}_{t_1}, \mathbf{q}_{t_1}\right) \\ \vdots \\ \boldsymbol{\phi}\left(\ddot{\mathbf{q}}_{t_S}, \dot{\mathbf{q}}_{t_S}, \mathbf{q}_{t_S}\right) \end{bmatrix} \boldsymbol{\pi} = \boldsymbol{\Phi}_S \boldsymbol{\pi}, \tag{2}$$

where $\boldsymbol{\Phi}_S$ is the trajectory full regressor matrix. Actually, experimental sampling $\widetilde{\mathbf{T}}$ and $\widetilde{\boldsymbol{\Phi}}$ includes also measurements noise, so that eq. (2) is expressed as:

$$\widetilde{\mathbf{T}}_S = \widetilde{\boldsymbol{\Phi}}_S \hat{\boldsymbol{\pi}} + \mathbf{v}, \quad \mathbf{v} \sim \mathcal{N}(0, \sigma_\nu). \tag{3}$$

[1] *COMAU ORL library* (COMAU Robotics, 2010) has been used for the motion interpolation.

Several techniques are known (Benimeli et al., 2006) for a pseudo-inversion solution of eq. (3). The weighted least-squares technique as in (Gautier, 1997) has been here implemented. Denoting $\boldsymbol{W}$ as a suitable weight matrix (computed from the standard deviation of measured torques), the system is solved as:

$$\hat{\boldsymbol{\pi}} = \left[(\widetilde{\boldsymbol{\Phi}}_S^t \boldsymbol{W} \widetilde{\boldsymbol{\Phi}}_S)^{-1} \widetilde{\boldsymbol{\Phi}}_S^t \boldsymbol{W} \right] \widetilde{\mathbf{T}}_S. \tag{4}$$

3 DECOUPLED DYNAMICS IDENTIFICATION

The method here presented implements a GA for the identification of "best" exciting trajectories. The fitness function provides two terms similarly to what proposed in (Presse and Gautier, 1993): one proportional to the logarithm of the determinant of $\det\left(\boldsymbol{\Phi}_S^t \boldsymbol{\Phi}_S\right)$, and one proportional to the coupling index introduced in the next Section.

3.1 Dynamics Coupling Evaluation Index over Trajectory

A metric for the evaluation of the coupling effects along all the path can be straightforwardly derived from the analysis of conditioning number of the covariance. From eq. (2), and under the assumption that the regression matrix $\boldsymbol{\Phi}$ is built with a trajectory free of noise, and that the torque measurements provides zero-mean uncorrelated noise, the variance of the EP results:

$$\boldsymbol{\sigma}_\pi^2 = \boldsymbol{\Phi}^+ \boldsymbol{\sigma}_T^2 \boldsymbol{\Phi}^{+^t}$$

Assuming the same variance value σ_n for the measure of each motor torque such that $\boldsymbol{\sigma}_T^2 = \sigma_n^2 \boldsymbol{I}$, the relation can be simplified as follow:

$$\begin{aligned} \boldsymbol{\sigma}_\pi^2 &= \boldsymbol{\Phi}^+ \boldsymbol{\sigma}_T^2 \boldsymbol{\Phi}^{+^t} = \sigma_n^2 \boldsymbol{\Phi}^+ \boldsymbol{\Phi}^{+^t} = \sigma_n^2 (\boldsymbol{\Phi}^t \boldsymbol{\Phi})^{-1} \\ &= \sigma_n^2 \boldsymbol{\Psi}, \end{aligned}$$

where the matrix $\boldsymbol{\Psi}$ has been introduced for sake of simplicity. Notably, as a difference from eq. (4), no weight is applied. Optimal design of the experiment should correspond to get the matrix $\boldsymbol{\Psi}$ equal to diagonal matrix. Finally, denote the *coupling-index* as:

$$I_c = \sum_{i=1}^{N_\pi} \sum_{j>i}^{N_\pi} \frac{|\psi_{i,j}|}{\sqrt{\psi_{i,i}\,\psi_{j,j}}}. \tag{5}$$

Each element of the sum are normalized within $[0,1]$. In addition, if the two parameters i and j are un-correlated the value of $\psi_{i,j}$ is zero.
Notably, $I_c = 0$ corresponds to a diagonal system, and, thus, it exists a properly scaled system such that the conditioning number is equal to 1, *i.e.* $\mathrm{cond}\left(\boldsymbol{\Phi}\,\mathrm{diag}\left(\lambda_1,\ldots,\lambda_{N_\pi}\right)\right) = 1$. However, the definition of the proper scaling factors λ_i needs a good *a priori* knowledge of EP (Presse and Gautier, 1993). In addition, I_c is mathematically simpler and less sensitive to numerical issues to be calculated than the conditioning number for trajectories with many thousands of points.

3.2 Comparison of Trajectories with Different Samples Number

Consider eq. (2) and hypothesize to resample the trajectory adding some other S points temporarily each one near one of the previous points. Thus:

$$\mathbf{T}_{2S} = \begin{bmatrix} \boldsymbol{\phi}\left(\ddot{\mathbf{q}}_{t_1}, \dot{\mathbf{q}}_{t_1}, \mathbf{q}_{t_1}\right) \\ \vdots \\ \boldsymbol{\phi}\left(\ddot{\mathbf{q}}_{t_S}, \dot{\mathbf{q}}_{t_S}, \mathbf{q}_{t_S}\right) \\ \boldsymbol{\phi}\left(\ddot{\mathbf{q}}_{t_1+dt}, \dot{\mathbf{q}}_{t_1+dt}, \mathbf{q}_{t_1+dt}\right) \\ \vdots \\ \boldsymbol{\phi}\left(\ddot{\mathbf{q}}_{t_S+dt}, \dot{\mathbf{q}}_{t_S+dt}, \mathbf{q}_{t_S+dt}\right) \end{bmatrix} \boldsymbol{\pi} = \boldsymbol{\Phi}_{2S} \boldsymbol{\pi},$$

with $\boldsymbol{\phi}\left(\ddot{\mathbf{q}}_{t_k}, \dot{\mathbf{q}}_{t_k}, \mathbf{q}_{t_k}\right) \simeq \boldsymbol{\phi}\left(\ddot{\mathbf{q}}_{t_k+dt}, \dot{\mathbf{q}}_{t_k+dt}, \mathbf{q}_{t_k+dt}\right)$. It is easy to demonstrate that

$$\boldsymbol{\Phi}_{2S}^t \boldsymbol{\Phi}_{2S} \simeq 2 \boldsymbol{\Phi}_S^t \boldsymbol{\Phi}_S$$

and, consequently, the determinant results:

$$\det\left(\boldsymbol{\Phi}_{2S}^t \boldsymbol{\Phi}_{2S}\right) \simeq \det\left(\boldsymbol{\Phi}_S^t \boldsymbol{\Phi}_S\right) 2^{N_\pi}.$$

In general, if any point generates k points we get

$$\det\left(\boldsymbol{\Phi}_{kS}\right) \simeq k^{N_\pi} \det\left(\boldsymbol{\Phi}_S^t \boldsymbol{\Phi}_S\right).$$

Finally, if $N \gg N_\pi$ in general the determinant of $\boldsymbol{\Phi}_N^t \boldsymbol{\Phi}_N$ evaluated on N points is

$$\det\left(\boldsymbol{\Phi}_N^t \boldsymbol{\Phi}_N\right) = a N^{N_\pi} \quad \rightarrow \quad a = \frac{\det\left(\boldsymbol{\Phi}_N^t \boldsymbol{\Phi}_N\right)}{N^{N_\pi}}$$

and so a can be used to compare trajectories sampled with different points.

3.3 Optimal Trajectory Identification

The template-class of trajectory for solving eq. (4) is directly provided by a real IR interpolator[2], as in (Villagrossi et al., 2013). The input for the algorithm is the trajectory interpolated (by motion planner functions, MP) from a set of K target via-points in the joint space:

$$MP\left(\overline{\mathbf{q}}_1,\ldots,\overline{\mathbf{q}}_K\right). \tag{6}$$

[2]Many robot producers offer libraries compliant to RCS standard (Vollmann, 2002) and fork.

Table 1: GA results (120 generation). N is the samples number. The I_c for algorithm A has been calculated a posteriori.

	N	$\log_{10}\left\|\frac{\det(\mathbf{H}^t\mathbf{H})}{N^{N_\pi}}\right\|$	I_c	Notes
A	2000	90.5	127.9	Eq. (8) in Appendix: $W=3$; $\boldsymbol{\omega}_{max}=[0.94,2.38,0.53,0.44,0.89,0.44]$ and $\boldsymbol{\omega}_{min}=[0.314,0.314,0.314,0.314,0.314]$. GA configuration: number of individuals=100, mutation=0.01, cross-over rate=0.7. Time duration of optimization process less than 1 s for each individual.
B	15996	30.9	101.2	Eq. (7): $\lambda_1=0.7$, and $\lambda_2=0.3$. Eq. (6): $K=6$. GA configuration: number of individuals=150, mutation=0.01, cross-over rate=0.9. Time duration of optimization process less than 1s for each individual.

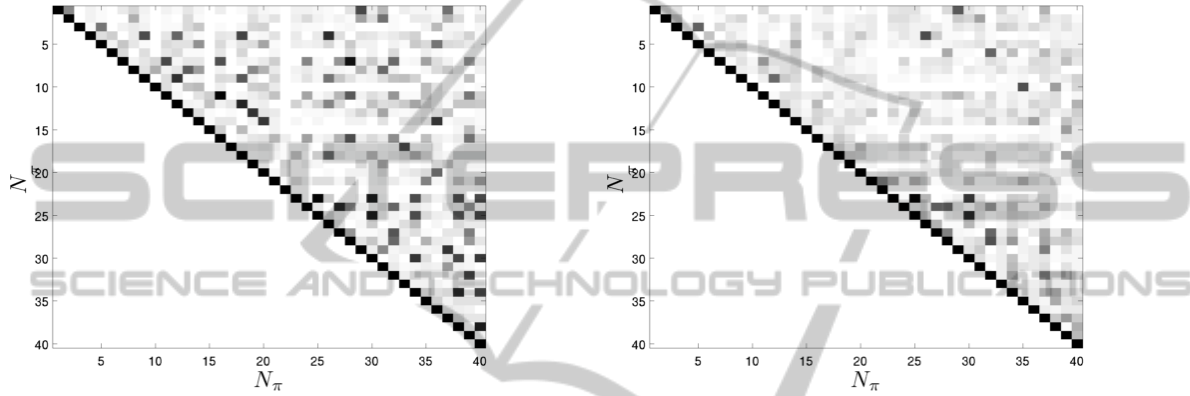

(a) (b)

Figure 2: The figures represent the plot of *correlation-matrix* defined in equation eq. (5). Black elements are equal to 1 while color shade to white for elements equal to 0. In figure (a) is shown matrix $\psi_{i,j}/\sqrt{\psi_{i,i}\psi_{j,j}}$ obtained from algorithm A while in figure (b) is shown $\psi_{i,j}/\sqrt{\psi_{i,i}\psi_{j,j}}$ matrix obtained from algorithm B. The plot exclude the term related to the friction.

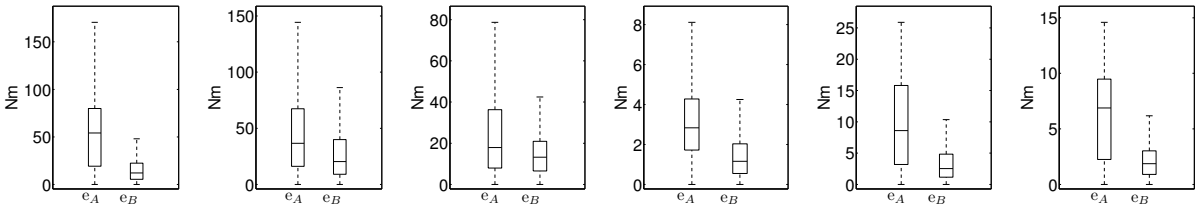

(Ax. 1) (Ax. 2) (Ax. 3) (Ax. 4) (Ax. 5) (Ax. 6)

Figure 3: Mean error in the torque prediction calculated over 30 randomly wide trajectories covering the whole workspace. The central mark is the median, the edges of the box are the 25th and 75th percentiles, the whiskers extend to the most extreme data points the algorithm considers to be not outliers. Trajectories have been generated from the IR Motion Planner.

Individual genomes in the GA are therefore the coordinates of the K via-points and each joint maximum velocity. The selection of individuals is made on a two-weighted terms fitness function: the first term is the D-optimal metric defined in equation eq. (9) and the second term is the coupling index I_c in eq. (5):

$$f=\lambda_1\log_{10}\left|\frac{\det\left(\tilde{\boldsymbol{\Phi}}^t\tilde{\boldsymbol{\Phi}}\right)}{N^{N_\pi}}\right|+\lambda_2\frac{I_{c_{max}}}{I_c} \qquad (7)$$

where $I_{c_{max}}$ is the maximum value of coupling-index, *i.e.* $I_{c_{max}}=N_\pi\times(N_\pi-1)/2$. Fitness terms are normalized so to consistently weight their contributions through λ_1 and λ_2 in $[0,1]$ such that $\lambda_1+\lambda_2=1$. A trial-and-error procedure has been applied for the optimal definition of the value of λ_1 and λ_2.

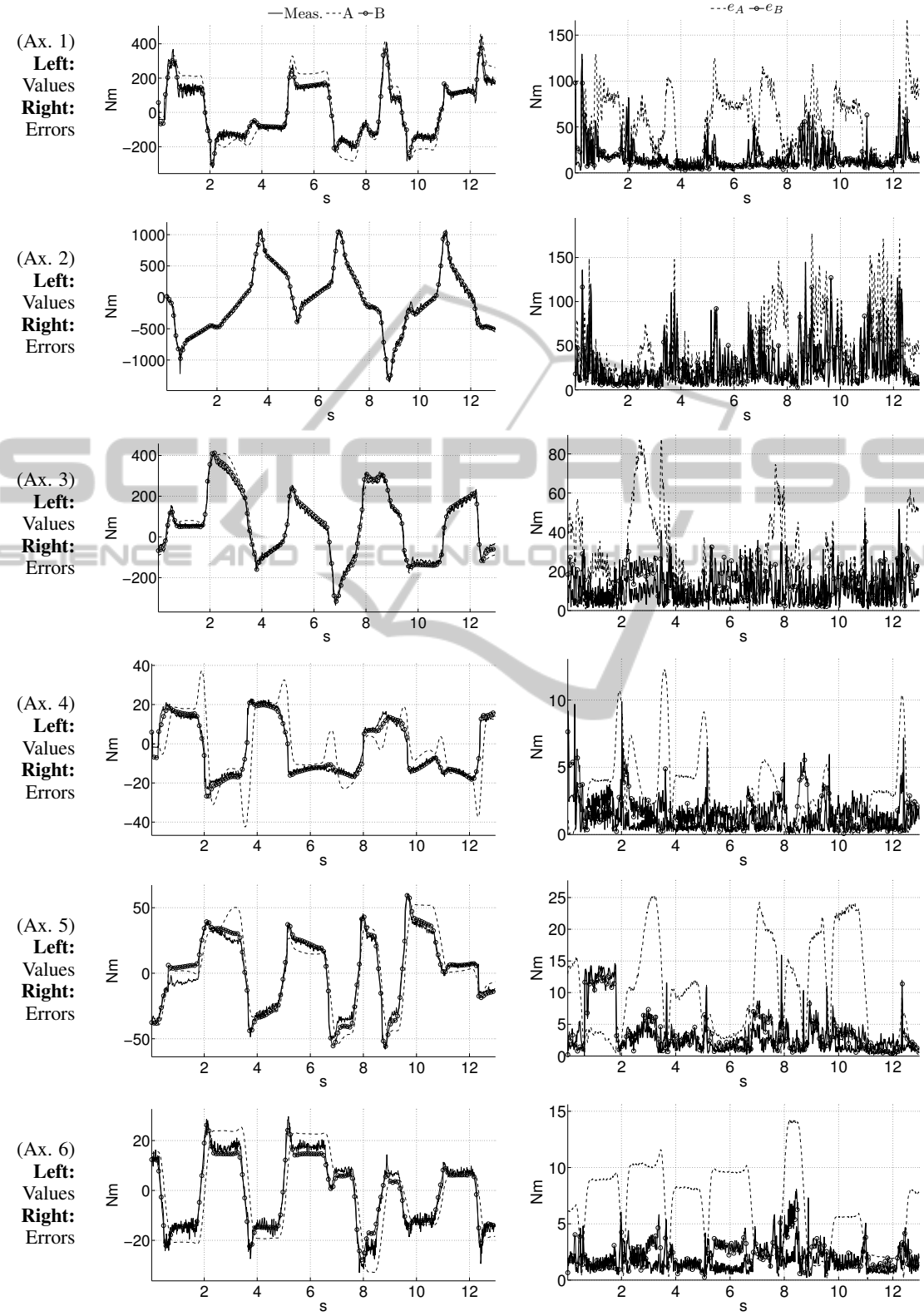

Figure 4: Value Measured and Estimated with the two Algorithms A, B for the execution of one sample trajectory of the set are shown (low pass filter, $30Hz$).

Table 2: Parameters list as in (Villagrossi et al., 2013), an extension of (Antonelli et al., 1999) considering also the 18 parameters of the friction model. π_C are the data provided from COMAU: from 1 to 40 are the CAD data, while from 41 to 58 are the identified friction values (the parameter from 53 to 58 are zero because COMAU has a linear model of the friction). COMAU declares a not negligible inaccuracy in the link weight about the 5%-10%.

Par. Id	Par. Symb	$\hat{\pi}_A^*$	$\hat{\pi}_B^*$	π_C	Par. Id	Par. Symb	$\hat{\pi}_A^*$	$\hat{\pi}_B^*$	π_C
1	mc_{2y}	1.285	0.499	-0.230	2	I_{2xy}	-2.241	1.243	0.095
3	I_{2yz}	-9.113	1.649	-0.053	4	I_{3xy}	-0.659	1.074	0.100
5	I_{3yz}	-7.984	0.630	-0.014	6	I_{3m}	15.465	15.765	10.480
7	mc_{4x}	0.465	-0.070	-0.001	8	I_{4xy}	-0.038	-0.521	0.000
9	I_{4xz}	-1.377	0.295	-0.000	10	I_{4m}	-6.308	0.878	0.253
11	mc_{5x}	-0.086	0.020	0.000	12	I_{5xy}	-2.080	-0.036	-0.000
13	I_{5xz}	-2.840	-0.029	0.000	14	I_{5yz}	0.121	0.071	-0.000
15	I_{5m}	-0.751	3.059	0.298	16	mc_{6x}	0.186	-0.101	0.001
17	mc_{6y}	-0.035	0.056	0.000	18	I_{6xy}	-0.036	-0.023	-0.000
19	I_{6xz}	-0.901	-0.029	-0.000	20	I_{6yz}	-0.040	0.023	-0.000
21	I_{6zz}	0.404	0.029	0.001	22	I_{6m}	-2.091	1.527	0.120
23	$I_{1yy}+I_{1m}+0.090\,m_2+I_{2yy}+0.580\,m_3+I_{3zz}+0.614\,m_4+0.614\,m_5+0.614\,m_6$						86.800	96.898	79.979
24	$mc_{2x}+0.700\,m_3+0.700\,m_4+0.700\,m_5+0.700\,m_6$						71.988	71.148	65.056
25	$I_{2xx}-I_{2yy}-0.490\,m_3-0.490\,m_4-0.490\,m_5-0.490\,m_6$						-50.268	-55.411	-45.728
26	$I_{2xz}+0.700\,mc_{3y}$						-3.903	-4.422	2.952
27	$I_{2zz}+I_{2m}+0.490\,m_3+0.490\,m_4+0.490\,m_5+0.490\,m_6$						102.833	112.234	71.700
28	$mc_{3x}+0.185\,m_4+0.185\,m_5+0.185\,m_6$						11.794	10.408	10.725
29	$mc_{3z}+mc_{4y}+0.624\,m_5+0.624\,m_6$						12.770	12.466	12.181
30	$I_{3xx}-I_{3zz}-0.034\,m_4+I_{4zz}+0.355\,m_5+0.355\,m_6$						15.805	6.938	2.685
31	$I_{3xz}-0.185\,mc_{4y}-0.115\,m_5-0.115\,m_6$						-1.053	-4.269	-1.606
32	$I_{3yy}+0.034\,m_4+I_{4zz}+0.423\,m_5+0.423\,m_6$						4.021	9.244	6.399
33	$mc_{4z}-mc_{5y}$						-0.036	-0.066	-0.061
34	$I_{4xx}-I_{4zz}+I_{5zz}$						-2.040	0.558	0.029
35	$I_{4yy}+I_{5zz}$						-1.725	-0.131	0.070
36	$I_{4yz}+0.624\,mc_{5y}$						-1.013	0.031	0.035
37	$mc_{5z}+mc_{6z}$	0.702	0.707	0.190	38	$I_{5xx}-I_{5zz}+I_{6yy}$	-1.990	-0.066	0.017
39	$I_{5yy}+I_{6yy}$	2.474	0.214	0.019	40	$I_{6xx}-I_{6yy}$	0.644	0.067	0.000
41	$f_{0,1}$	38.190	61.121	68.035	42	$f_{0,2}$	1.397	0.722	0.719
43	$f_{0,3}$	37.803	77.093	108.777	44	$f_{0,4}$	2.850	2.479	1.104
45	$f_{0,5}$	33.721	37.687	50.446	46	$f_{0,6}$	1.497	1.700	0.685
47	$f_{1,1}$	4.811	6.262	9.248	48	$f_{1,2}$	0.404	0.160	0.057
49	$f_{1,3}$	6.232	10.112	8.904	50	$f_{1,4}$	0.676	0.277	0.287
51	$f_{1,5}$	3.214	0.920	5.148	52	$f_{1,6}$	1.117	0.228	0.155
53	$f_{2,1}$	-0.005	-0.000	–	54	$f_{2,2}$	-0.009	-0.003	–
55	$f_{2,3}$	-0.004	-0.003	–	56	$f_{2,4}$	-0.010	-0.001	–
57	$f_{2,5}$	-0.009	-0.001	–	58	$f_{2,6}$	-0.128	-0.001	–

4 EXPERIMENTS AND DISCUSSION

4.1 Design of Experiment

The experimental setup includes a COMAU NS16 manipulator, with C4GOpen controller option and the *Open Realistic Robot Library*. No payload has been attached. The number of BP for this robot is equal to 43, while EP are 40 (Antonelli et al., 1999). In addition to inertial parameter, 3 friction parameters per axis have been considered, yielding a total of $N_\pi = 58$ parameters. The joint positions and the motor currents have been acquired at $1kHz$. The data have been filtered through approximated spline (MATLAB$^{(R)}$ command SPAPS) and tolerance has been set equal to the measure variance (calculated through *ad-hoc* experiment). Joint velocities and acceleration have been calculated as first and second analytical derivative of the so interpolated joint positions.

As a preliminary investigation of the validity of the approach, one of the most popular state-of-the-art methods, (Calafiore et al., 2001), has been implemented and compared experimentally to the one here proposed. For sake of brevity, "*A*" and "*B*" will be used to indicate the method from (Calafiore et al.,

2001) and the one here proposed respectively. The method *A* is shortly reported in the Appendix for sake of notation consistency.

4.2 Estimated Parameters

Table 1 reports the characteristics of the two optimal trajectories implemented from the results of the two algorithms *A* and *B*. As expected, *A* provides a higher-determinant trajectory, while its coupling index is poorer. The trajectory from *B*, in fact, achieves a much lower correlation influence among EP, see Figure 2. Both optimal trajectories have been then executed 30 times each, and the EP have been estimated in each repetition through eq. (4), so that the EP reported in Table 2 are the mean over the 30 repetitions of the 30 different random trajectories. Furthermore, in Table 2 the fourth column, indicated as π_C, lists the CAD data provided from the robot manufacturer from 1 to 40 and the friction values identified from COMAU from 41 to 58 (the parameters from 53 to 58 are zero because COMAU has a linear model of the friction). COMAU declares a not negligible variability in the link weight about the 5%-10% due to the inaccuracy of the casting process. Looking at parameters from 1 to 22 and from 33 to 58, the Algorithm *B* identifies values that are averagely closer to CAD (except parameter 3, 15 and 46). On the other hand, looking at the parameters from 23 to 32, that are the complex aggregates parameters, the Algorithm *A* identifies values averagely closer to CAD. This difference should derive from the numerical procedures used for the EP selection (Antonelli et al., 1999). Indeed, different thresholds may aggregate BP around different EP. This should indicate that the method here presented should be better applied to the identification of BP set introducing a priori knowledge of the system to overcome the issues on the observability. Future works will be done on this topic.

4.3 Torque Prediction Power

The prediction power of the estimated parameters has been validated by 30 different random test trajectories generated through the *ORL* library. The trajectories were wide, covering the entire workspace. The mean error in the torque prediction has been calculated for each repetition and for each axis. Figure 3 displays the statistics (median/quartile) of the distribution of mean error of each axis over the 30 repetitions. Figure 4 displays the results of joint torques reconstruction for one paradigmatic experiment. Averagely, the algorithm *B* provide lower prediction error for all axes.

5 CONCLUSION

The paper has introduced a novel index to estimate the average coupling of the trajectory in term of correlation among the essential parameters. Two different algorithm have been implemented and compared, testing their performances. Experimental results demonstrate how a decoupling trajectory produce a better estimation. Future works will focused on the propagation of the covariance taking into account that the dynamic regressor $\mathbf{\Phi}$ is not free of noise. Furthermore, a deep analysis of the physical meaning of the essential parameters will be investigated.

ACKNOWLEDGMENT

R. Bozzi, and J. C. Dalberto, laboratory technicians of CNR-ITIA, have been involved in setting up the experiments. This work is partially within FLEXICAST funded by FP7-NMP EC.

REFERENCES

Antonelli, G., Caccavale, F., and Chiacchio, P. (1999). A systematic procedure for the identification of dynamic parameters of robot manipulators. *Robotica*, 17(04):427–435.

Atkeson, C. G., An, C. H., and Hollerbach, J. M. (1986). Estimation of inertial parameters of manipulator loads and links. *Int J of Rob Res*, 5(3):101–119.

Benimeli, F., Mata, V., and Valero, F. (2006). A comparison between direct and indirect dynamic parameter identification methods in industrial robots. *Robotica*, 24(5):579–590.

Caccavale, F. and Chiacchio, P. (1994). Identification of dynamic parameters and feedforward control for a conventional industrial manipulator. *Control Engineering Practice*, 2(6):1039–1050.

Calafiore, G., Indri, M., and Bona, B. (2001). Robot dynamic calibration: Optimal excitation trajectories and experimental parameter estimation. *J. of Robotic Systems*, 18(2):55–68.

COMAU Robotics (2010). Open realistic robot library.

Gautier, M. (1997). Dynamic identification of robots with power model. In *Rob. and Aut., Proc., IEEE Int. Conf. on*, volume 3, pages 1922 –1927.

Gautier, M. and Khalil, W. (1988). On the identification of the inertial parameters of robots. In *Dec and Contr, Proc. of IEEE Conf. on*, volume 3, pages 2264 –2269.

Gautier, M. and Venture, G. (2013). Identification of standard dynamic parameters of robots with positive definite inertia matrix. In *Intell Rob and Sys, 2013 IEEE/RSJ Int Conf on*, pages 5815–5820.

Indri, M., Calafiore, G., Legnani, G., Jatta, F., and Visioli, A. (2002). Optimized dynamic calibration of a scara

robot. In *IFAC '02. 2002 IFAC Internation Federation on Automatic Control*.

Otani, K. and Kakizaki, T. (1993). Motion planning and modeling for accurately identifying dynamic parameters of an industrial robotic manipulator. In *Proc of the 24th Int Symp on Ind Rob*, pages 743–748.

Park, K. (2006). Fourier-based optimal excitation trajectories for the dynamic identification of robots. *Robotica*, 24(5):625–633.

Pham, C. M. (1991). Essential parameters estimation. *Dec and Contr, Proc of IEEE Conf on*, 2769(4):2769–2774.

Presse, C. and Gautier, M. (1993). New criteria of exciting trajectories for robot identification. In *Proc IEEE Int Conf on Rob and Aut*, pages 907–912.

Pukelsheim, F. (2006). *Optimal design of experiments*. The Society for Industrial and Applied Mathematics, New York.

Rackl, W., Lampariello, R., and Hirzinger, G. (2012). Robot excitation trajectories for dynamic parameter estimation using optimized b-splines. In *2012 IEEE Int. Conf. on Rob. and Aut.*, pages 2042–2047.

Swevers, J., Ganseman, C., Tukel, D., de Schutter, J., and Van Brussel, H. (1997). Optimal robot excitation and identification. *Rob and Aut, IEEE Tran on*, 13(5):730–740.

Villagrossi, E., Pedrocchi, N., Vicentini, F., and Molinari Tosatti, L. (2013). Optimal robot dynamics local identification using genetic-based path planning in workspace subregions. In *Adv Intell Mech, 2013 IEEE/ASME Int. Conf. on*, pages 932–937.

Vollmann, K. (2002). Realistic robot simulation: multiple instantiating of robot controller software. In *IEEE ICIT Industrial Technology*, volume 2, pages 1194–1198.

Wu, J., Wang, J., and You, Z. (2010). An overview of dynamic parameter identification of robots. *Robotics and Computer-Integrated Manufacturing*, 26(5):414–419.

APPENDIX

For sake of clarity, the Appendix reports a brief summary of the algorithm described in (Calafiore et al., 2001). Refers to the original paper for all the details. The template-class of trajectory used for the optimization is:

$$q^j = q_0^j + \sum_{k=1}^{W} a_k^j \sin\left(\omega_k^j t\right) \quad j = 1,\ldots,dof. \quad (8)$$

where q_0^j is the initial offset, a_k^j and ω_k^j is respectively the amplitude and the angular frequency of the sine. W is a small integer representing the maximum number of harmonics present in the signal. Collecting the free variables $\mathbf{a}_k = [a_k^1,...,a_k^{dof}]^t$ and $\boldsymbol{\omega}_k = [\omega_k^1,...,\omega_k^{dof}]^t$, the set of the decision variables of the optimization problem results $\{\mathbf{a}_1,\boldsymbol{\omega}_1,...,\mathbf{a}_W,\boldsymbol{\omega}_W\}$ and proper constraints are to be imposed coherently with the kinematics of the robot:

$$|a_k^j| < \frac{q_{max}^j}{W}, \quad \text{and} \quad |\omega_k^j| < \sqrt{\frac{\ddot{q}_{max}^j}{q_{max}^j}}, \quad j = 1,\ldots,dof.$$

The set of optimum parameters $\{\mathbf{a}_1^\star,\boldsymbol{\omega}_1^\star,...,\mathbf{a}_W^\star,\boldsymbol{\omega}_W^\star\}_A$ are obtained from the *GA*. The selection of individuals is made on the well-known *D*-optimal considering the maximization of the determinant of a quadratic form associated with $\boldsymbol{\Phi}^n$ of each n-th individual trajectory

$$f = \log_{10} \| \det\left[\boldsymbol{\Phi}'\boldsymbol{\Phi}\right] / N^{N_\pi} \|. \quad (9)$$

where N denotes the trajectory samples, and N_π the number of the essential parameters. The scaling of the determinant by the factor N^{N_π} has been introduced in order to allow the comparison between trajectories with different number of points.